Published in final edited form as:
Neuron. 2011 July 14; 71(1): 131–141. doi:10.1016/j.neuron.2011.05.033.

S-Nitrosylation and S-Palmitoylation Reciprocally Regulate Synaptic Targeting of PSD-95

Gary P. H. Ho[1], **Balakrishnan Selvakumar**[1], **Jun Mukai**[2], **Lynda D. Hester**[1], **Yuxuan Wang**[1], **Joseph A. Gogos**[2,3], and **Solomon H. Snyder**[1,4,5]

[1]Solomon H. Snyder Department of Neuroscience, Johns Hopkins University School of Medicine, Baltimore, MD

[2]Department of Physiology and Cellular Biophysics, College of Physicians & Surgeons, Columbia University, New York, NY

[3]Department of Neuroscience, College of Physicians & Surgeons, Columbia University, New York, NY

[4]Department of Pharmacology and Molecular Sciences, Johns Hopkins University School of Medicine, Baltimore, MD

[5]Department of Psychiatry and Behavioral Sciences, Johns Hopkins University School of Medicine, Baltimore, MD

Abstract

PSD-95, a principal scaffolding component of the post-synaptic density, is targeted to synapses by palmitoylation where it couples NMDA receptor stimulation to production of nitric oxide (NO) by neuronal nitric oxide synthase (nNOS). Here, we show that PSD-95 is physiologically S-nitrosylated. We identify cysteines 3 and 5, which are palmitoylated, as sites of nitrosylation, suggesting a competition between these two modifications. In support of this hypothesis, physiologically produced NO inhibits PSD-95 palmitoylation in granule cells of the cerebellum, decreasing the number of PSD-95 clusters at synaptic sites. Further, decreased palmitoylation, as seen in heterologous cells treated with 2-bromopalmitate or in ZDHHC8 knockout mice deficient in a PSD-95 palmitoyltransferase, results in increased PSD-95 nitrosylation. These data support a model in which NMDA mediated production of NO regulates targeting of PSD-95 to synapses *via* mutually competitive cysteine modifications. Thus, differential modification of cysteines may represent a general paradigm in signal transduction.

Introduction

PSD-95, the principal protein of post-synaptic densities (PSD), is a major scaffolding protein which impacts synaptic plasticity (Cho et al., 1992; Migaud et al., 1998). In addition to maintaining the molecular architecture of the PSD (Chen et al., 2008), PSD-95 enhances long-term depression (Stein et al., 2003) and is required for spatial learning in mouse models (Migaud et al., 1998). N-terminal palmitoylation targets PSD-95 to synapses, where it clusters AMPA-type glutamate receptors (Chen et al., 2000) and physically links NMDA

Correspondence: ssnyder@jhmi.edu (S.H.S.).

receptors to neuronal nitric oxide synthase (nNOS) (Brenman et al., 1996; Christopherson et al., 1999). This interaction enables calcium that permeates NMDA receptors to activate nNOS by binding calmodulin associated with the enzyme (Bredt and Snyder, 1990). Suppression of PSD-95 expression (Sattler et al., 1999) or inhibition of binding between PSD-95 and the NMDA receptor with exogenous peptides (Aarts et al., 2002) reduces NO mediated excitotoxicity, emphasizing the role of PSD-95 in transducing signals from the NMDA receptor to nNOS.

PSD-95 also regulates AMPA receptors through its interaction with stargazin (Chen et al., 2000). This binding is required for recruitment of AMPA receptors to the synapse (Schnell et al., 2002). Consistent with this observation, mice deficient in PSD-95 have decreased AMPA receptor mediated neurotransmission (Beique et al., 2006). Furthermore, appropriate interactions between PSD-95 and A Kinase-Anchoring Protein (AKAP) are required for NMDA mediated AMPA receptor endocytosis (Bhattacharyya et al., 2009).

PSD-95 function is regulated by dynamic cycling of palmitoylation and depalmitoylation (El-Husseini Ael et al., 2002). Glutamate receptor activation enhances depalmitoylation of PSD-95 (El-Husseini Ael et al., 2002), while blockade of synaptic activity enhances PSD-95 palmitoylation through regulated translocation of the dendritic palmitoyl acyltransferase (PAT) DHHC2 (Noritake et al., 2009). Palmitoylation influences synaptic dynamics by augmenting clustering of PSD-95 at dendritic spines (Craven et al., 1999).

Palmitoylation of PSD-95 takes place at cysteines 3 and 5 (Topinka and Bredt, 1998). Nitric oxide signals in large part by S-nitrosylating (hereafter referred to as `nitrosylating') cysteines in a variety of proteins (Hess et al., 2005). Hess et al (Hess et al., 1993) showed that NO donors can inhibit the palmitoylation of several proteins in dorsal root ganglia neurons and suggested that an NO mediated post-translational modification might compete with palmitoylation. Due to its close physical proximity to both the NMDA receptor and nNOS, we wondered whether PSD-95 might be a target for nitrosylation and whether there might be some interaction between putative nitrosylation and palmitoylation of PSD-95. In the present study we show that PSD-95 is physiologically nitrosylated at cysteines 3 and 5 in a reciprocal relationship with palmitoylation. This process impacts the physiologic clustering of PSD-95 at synapses.

Results

PSD-95 is physiologically nitrosylated at cysteines 3 and 5

We examined the possibility that PSD-95 can be nitrosylated by exposing HEK293 cells containing overexpressed PSD-95 to the NO donor cysteine-NO (Cys-NO) (Figure 1A). The NO donor elicits nitrosylation of PSD-95, monitored by the biotin switch assay, in a concentration-dependent fashion. To determine whether PSD-95 is physiologically nitrosylated in mammalian brain, we monitored endogenous PSD95 in mouse brain from wild-type and nNOS deleted animals (Figure 1B). We observe ascorbate-dependent basal nitrosylation of endogenous PSD-95 which is abolished in nNOS knockout mice. Levels of nitrosylated PSD-95 are comparable to those of the NR2A subunit of the NMDAR (Figure 1C).

PSD-95 is palmitoylated at cysteines 3 and 5 (Topinka and Bredt, 1998). These occur in the N-terminal 60% of the protein which contains the three PDZ domains that are sufficient for synaptic targeting in the context of endogenous PSD-95 expression (Craven et al., 1999; Sturgill et al., 2009). While PSD-95 contains six cysteines, only two of these (C3 and C5) occur in the N-terminal (amino acids 1-433) fragment, which we designate PSD-95-1-433. We observe similar levels of nitrosylation for full-length PSD-95 and PSD-95-1-433 in

HEK-nNOS cells (Figure 1D). In HEK-nNOS cells nitrosylation of PSD-1-433 is abolished with mutation of both C3 and C5 with intermediate effects in the individual C3 and C5 mutants (Figure 1E).

Palmitoylation of PSD-95 is physiologically regulated by NO

Since PSD-95 is palmitoylated and nitrosylated at the same cysteines, we wondered whether the two processes might be mutually competitive. Consistent with this hypothesis, stable overexpression of nNOS in HEK293 cells substantially diminishes palmitoylation of full length PSD-95 as measured by [H]palmitate incorporation (Figure 2A). Inhibition of nNOS in these cells by the nNOS selective inhibitor L-VNIO (N5-(1-imino-3-butenyl)-L-ornithine) increases PSD-95 palmitoylation, while transient expression of nNOS in 293 cells reduces PSD-95 palmitoylation when measured directly by the acyl biotin exchange (ABE) procedure (Figure 2B, C). This method is analogous to the biotin switch method but uses hydroxylamine to reverse palmitoylation (Drisdel et al., 2006).

To confirm that NO is the mediator of these effects, we treated 293 cells with Cys-NO which markedly reduces [H]palmitate incorporation into PSD-95 (Figure 2D). NO donor treatment similarly reduces palmitoylation of PSD-95-1-433. The action of NO upon PSD-95 palmitoylation is selective. Thus, HRas is physiologically palmitoylated and nitrosylated, but the two processes occur at different sites of the protein (Hancock et al., 1989; Lander et al., 1996). NO donor treatment fails to alter palmitoylation of HRas (Figure 2E).

We explored the influence of NO upon palmitoylation of PSD-95 in mammalian brain. In both cerebellar granule and hippocampal cultures, palmitoylation, monitored with [H]palmitate, is virtually abolished by NO donor treatment (Figure 3A, B) concomitant with increases in PSD-95 nitrosylation (Figure 3C, D).

We wondered whether endogenous NO regulates palmitoylation of PSD-95 in the brain. Since nNOS is highly expressed in granule cells of the cerebellum, we chose to focus on this system. Utilizing the ABE assay in cerebellar granule cells, we detect robust palmitoylation of endogenous PSD-95 which is significantly enhanced by treatment with L-VNIO (Figure 3E). Thus, endogenous NO physiologically diminishes levels of PSD-95 palmitoylation.

Blocking synaptic activity with tetrodotoxin (TTX) increases palmitoylation of several proteins including PSD-95 (Hayashi et al., 2009; Noritake et al., 2009). Nitrosylation of PSD-95 is decreased and palmitoylation increased in neurons treated with TTX (Figure 3F, G).

NMDAR mediated neurotransmission is known to stimulate NO formation (Bredt and Snyder, 1989). We conducted experiments to assess its impact on palmitoylation. NMDA treatment of granule cells reduces palmitoylation of PSD-95 by about 70% (Figure 2H). This action reflects NMDA augmentation of NO formation, as it is largely reversed by treatment with L-VNIO. Moreover, we observe reciprocal changes in PSD-95 nitrosylation, suggesting that nitrosylation is responsible for the effects of NMDA-mediated NO formation (Figure 3I). To further explore the importance of endogenous NO in regulating PSD-95 palmitoylation, we made use of nNOS deleted mice (Figure 3J). We confirm the marked reduction of PSD-95 palmitoylation in response to NMDA treatment. Levels of PSD-95 palmitoylation are significantly augmented in nNOS deleted granule cells both in the absence and presence of NMDA treatment (Figure 3J). NMDA does elicit some decrease in PSD-95 palmitoylation in nNOS knockout mice, which may reflect the retention of alternatively spliced, catalytically active nNOS (Eliasson et al., 1997) or compensatory mechanisms involving eNOS or iNOS (Huang and Fishman, 1996). Thus, diverse

experimental approaches establish that in mammalian brain endogenous NO under basal conditions and in response to NMDAR mediated neurotransmission regulates the palmitoylation of PSD-95.

Synaptic clustering of PSD-95 is inhibited by NMDA transmission in an NO dependent fashion

One of the principal roles of PSD-95 palmitoylation is to regulate synaptic clustering of the protein. Thus, synaptic clustering of PSD-95 is abolished with C3, 5 mutation which prevents palmitoylation (Craven et al., 1999). Moreover, inhibition of palmitoylation with 2-bromopalmitate (2-BP) reduces PSD-95 synaptic clusters (El-Husseini Ael et al., 2002). Bredt, Nicoll and Fukata established that glutamate neurotransmission, acting via ionotropic receptors, diminishes PSD-95 clustering both by inhibiting palmitoylation (Noritake et al., 2009) and stimulating depalmitoylation (el-Husseini Ael and Bredt, 2002). We wondered whether this process might involve influences of NO, acting by displacing palmitate from PSD-95. Accordingly, we examined the effect of NMDA treatment upon PSD-95 clustering in cerebellar granule neurons and evaluated the influence of the nNOS inhibitor VNIO (Figure 4). PSD-95 is synaptic in localization as it is closely apposed to clusters of synapsin, a pre-synaptic marker, with statistically significant co-localization (Pearson correlation coefficient, 0.45) (Figure 4A). NMDA treatment reduces PSD-95 synaptic clusters by about 40%, while VNIO significantly reverses this action. In contrast, synapsin clusters are unchanged. The partial reversal by VNIO may indicate that the NMDA effects involve other signaling systems in addition to NO, possibly associated with calcium entering cells through NMDA channels. Double labeling is specific, as demonstrated by omission of primary antibodies (Figure 5C). As previously reported, 2-BP reduces PSD-95 clustering (Figure 5A, B).

Palmitoylation of PSD-95 regulates basal AMPA receptor clustering (El-Husseini Ael et al., 2002). Addition of NMDA to cultured neurons triggers AMPA receptor endocytosis (Beattie et al., 2000). Treatment with 2-BP does not further decrease GluR2 surface clusters in neurons exposed to NMDA (Figure 4C, D), suggesting that palmitoylated targets including PSD-95 play a role in both basal and NMDA dependent AMPA receptor surface clustering.

These experiments establish that NMDAR mediated neurotransmission regulates PSD-95 clustering. The reduction of PSD-95 clustering in response to glutamatergic transmission involves NO. The regulation of PSD-95 clustering by NO reflects its influence upon palmitoylation of PSD-95.

Palmitoylation physiologically regulates nitrosylation of PSD-95

Nitrosylation is increasingly appreciated as a major post-translational modification of proteins (Cho et al., 2009; Hess et al., 2005; Whalen et al., 2007). Besides nitrosylation and palmitoylation, cysteines of proteins are physiologically modified by oxidative mechanisms involving hydrogen peroxide and other agents, as well as by glutathionylation, sulfhydration, and the formation of disulfide bonds. With the exception of disulfides (Takahashi et al., 2007), thus far there has been no evidence for physiologic regulation of nitrosylation by these other post-translational modifications of cysteines. We asked whether palmitoylation might normally modulate levels of nitrosylated PSD-95. In HEK-nNOS cells nitrosylation of PSD-95-1-433 is demonstrable and is lost with mutation of C3 and C5 (Figure 6A). Nitrosylation of PSD-95-1-433 is substantially augmented by treatment with 2-BP, indicating that endogenous palmitoylation reduces levels of PSD-95 nitrosylation. This reciprocity of nitrosylation and palmitoylation is selective. Thus, β-tubulin is known to be nitrosylated (Jaffrey et al., 2001) but has not been conclusively shown to be palmitoylated *in vivo*. Nitrosylation of tubulin is unaffected by 2-BP.

To assess whether endogenous palmitoylation of PSD-95 physiologically regulates its nitrosylation in intact animals, we examined brains of mice with targeted deletion of the palmitoyl acyltransferase enzyme ZDHHC8, which has been demonstrated to be a physiologic PAT for PSD-95 (Mukai et al., 2008) (Figure 6B). Levels of nitrosylation of PSD-95 are increased threefold in the ZDHHC8 knockout brains. By contrast, nitrosylation of GAPDH, which is not physiologically palmitoylated, is unaltered in the mutant mice. The proportionally larger increase in nitrosylation of PSD-95 compared to palmitoylation may be due to higher levels of palmitoylated PSD-95 in unstimulated brains with low basal levels of NO. A small change in palmitoylation may therefore result in a larger percentage change in nitrosylation of PSD-95. Neither palmitoylation (Hayashi et al., 2009) nor nitrosylation (Choi et al., 2000) of NR2A, which occur on distinct cysteines, is affected in the mutant mice (Figure 6C). Thus, nitrosylation of PSD-95 is physiologically modulated by palmitoylation.

NO is known to regulate NMDA receptors in a feedback fashion, inhibiting their function by nitrosylating them (Choi et al., 2000). PSD-95 serves as a conduit for NMDA receptors to activate nNOS, generating NO (Christopherson et al., 1999). We wondered whether the generated NO might feed back to regulate palmitoylation of PSD-95 through nitrosylation. Accordingly, we examined the binding of NR2B to PSD-95 in mice with ZDHHC8 deletion to determine whether higher levels of nitrosylated PSD-95 present in these mutant mice are associated with decreased NR2B-PSD-95 binding (Figure 6D). This binding is substantially reduced in the mutant mice. While deficient palmitoylation and mislocalization of PSD-95 may be involved in the decreased binding (Li et al., 2003), our results are consistent with the hypothesized feedback model.

Discussion

NO is well established as a modulator of synaptic transmission throughout the brain (Bredt, 1999). PSD-95, the principal component of post-synaptic densities, is a scaffolding protein influencing synaptic transmission. PSD-95 binds nNOS facilitating the linkage of NMDAR mediated neurotransmission to activation of nNOS by calcium that passes through NMDA ion channels (Christopherson et al., 1999; Sattler et al., 1999). Heretofore there has been no evidence for any reciprocal influence of NO upon PSD-95. Our study provides compelling evidence that NO physiologically nitrosylates PSD-95. Synaptic clustering of PSD-95, a process which determines its influence upon synaptic transmission, is critically dependent upon its palmitoylation (Craven et al., 1999). Our observation that nitrosylation and palmitoylation of PSD-95 are reciprocal events indicates that NO normally impacts major functions of PSD-95. We also observed that palmitoylation physiologically regulates nitrosylation of PSD-95.

Bredt, Nicoll and associates (El-Husseini Ael et al., 2002) have established that glutamatergic transmission leads to the depalmitoylation of PSD-95 with attendant influences upon synaptic events. Their studies did not indicate a specific molecular mechanism whereby glutamate transmission enhances depalmitoylation. Noritake and colleagues (Noritake et al., 2009) presented evidence for inhibition of palmitoylation by translocation of the DHHC2 PAT out of the PSD. Our study provides a well defined mechanism linking glutamatergic transmission and palmitoylation. Glutamate-NMDA neurotransmission leads to depalmitoylation of PSD-95 as reported by Bredt and colleagues (El-Husseini Ael et al., 2002). Calcium, entering cells via the NMDA ion channel, binds to calmodulin associated with nNOS causing NO formation. Generated NO nitrosylates PSD-95 in a process competitive with palmitoylation, blocking free cysteines and maintaining PSD-95 in the depalmitoylated state. Augmented NMDA transmission and associated NO formation thereby lead to decreased palmitoylation of PSD-95.

We have also shown that this regulation is reciprocal. While NO inhibits palmitoylation, endogenous palmitoylation also regulates nitrosylation of PSD-95. We demonstrate that deletion of a PSD-95 PAT, ZDHHC8, results in increased nitrosylation of PSD-95 concomitant with a decrease in binding of PSD-95 and NR2B. It is unknown whether or not ZDHHC8 has activity towards NR2B. Thus the potential contribution of altered NR2B palmitoylation in the ZDHHC8−/− mouse to decreased binding with PSD-95 remains to be clarified. ZDHHC8 is primarily localized in a perinuclear domain and in dendritic shafts of mature neurons with partial co-localization with PSD-95 at these sites (Mukai et al., 2008; Mukai et al., 2004).

Several depalmitoylating enzymes have been described, including APT1 and PPT1 (Fukata and Fukata, 2010). None of them has been shown to act upon PSD-95 directly. Thus, their role in regulating PSD-95 palmitoylation is unclear. Conceivably such depalmitoylating enzymes might act in conjunction with NO to influence the state of palmitoylation of PSD-95.

The modulation of PSD-95 palmitoylation by glutamatergic transmisson is reversed by CNQX, a drug that blocks AMPA receptors, and by AP5, an inhibitor of NMDA receptors, as well as by kynurenic acid, which blocks both ionotropic glutamate receptors (El-Husseini Ael et al., 2002). From these limited experiments one cannot assess the relative contribution of various subtypes of ionotropic glutamate receptors to the palmitoylation process. Moreover, there are no data available regarding the impact of metabotropic glutamate transmission upon PSD-95 palmitoylation. Our experiments emphasize the role of NMDA transmission in PSD-95 palmitoylation. Clarification of the detailed interaction of various types of glutamate transmission in influencing the counterbalance of NO and palmitoylation for regulation of PSD-95 awaits further investigation.

There is precedent for competing post-translational modifications influencing protein function, most notably with acetylation and ubiquitination (Ge et al., 2009; Giandomenico et al., 2003; Gronroos et al., 2002). Thus, the dynamic reciprocity between palmitoylation and nitrosylation of PSD-95 may reflect a process that occurs with other proteins that are nitrosylated and palmitoylated at the same sites. Nitrosylation is a very common post-translational modification affecting more than 100 proteins (Hess et al., 2005). Palmitoylation is similarly prevalent with at least 68 proteins in mammalian brain known to be palmitoylated plus an additional 200 candidates recently found in a proteomic screen (Kang et al., 2008). We are not aware of other studies in which reciprocal nitrosylation and palmitoylation have been characterized for individual proteins at the same sites. Because of the large numbers of proteins that are nitrosylated and/or palmitoylated, we suspect that interactions between these two processes are frequent and mediate numerous physiologic processes both in the brain and periphery.

Sulfhydration, a posttranslational modification elicited by the gasotransmitter actions of H S (Mustafa et al., 2009) also might influence PSD-95. H S signaling via sulfhydration differs in some respects from nitrosylation. A more stable modification, sulfhydration often activates proteins, because the SH becomes an even more reactive SSH, while nitrosylation often inactivates a reactive cysteine by converting the reactive SH to SNO. Whether putative sulfhydration of PSD-95 would functionally alter the protein differently than nitrosylation is unclear.

PSD-95 exerts its physiologic effects by binding to a variety of protein partners. Conceivably, nitrosylation of PSD-95 affects such binding. For instance, AKAP (A-kinase anchoring protein) links PSD-95 to AMPA receptor endocytosis (Bhattacharyya et al., 2009). NMDA neurotransmission, via nitrosylation of PSD-95, might impact interactions

with AKAP and provide another means of linking NMDA and AMPA receptors. Similarly, stargazin, which is physiologically nitrosylated (Selvakumar et al., 2009), binds to PSD-95 as well as AMPA receptors. Nitrosylation of PSD-95 might influence its binding to stargazin and thereby to AMPA receptors. Nitrosylation of stargazin facilitates its augmentation of the surface expression of AMPA receptors (Selvakumar et al., 2009). One might speculate that NMDA transmission would enhance nitrosylation of both PSD-95 and stargazin with complex influences upon AMPA receptor disposition.

Experimental Procedures

Cell Culture

HEK293 and HEK-nNOS cells were cultured in DMEM with FBS (10%), penicillin-streptomycin (2%), L-glutamine (2 mM) and tylosin (8 g/mL) (Sigma-Aldrich). Dissociated granule cells were prepared from mouse cerebellum as described (Kato et al., 2007) and plated at a density of 5 × 10 cells per 6 cm dish. Dissociated hippocampal neurons were prepared from E18 mice as described (Kang et al., 2010). For NMDA treatments prior to ABE analysis, cells with or without 1 hr of L-VNIO pre-treatment were stimulated with 300 μM NMDA and 10 μM glycine for 10 min in ACSF (in mM: 10 HEPES, 10 D-glucose, 2 CaCl , 3 KCl, 124 NaCl, pH 7.4) and returned to growth media for 8 hr. For basal L-VNIO treatments, 75 μM L-VNIO was added to growth media for 8 hr.

Antibodies and Reagents

Antibodies were purchased from the following companies: PSD-95 (7E3-1B8), Millipore for biochemistry, with the exception of Figure 3G, where PSD-95 (6G6 1C9, Millipore) was used; PSD-95 (MA1-046), Affinity Bioreagents for immunostaining; GADPH, Santa Cruz (rabbit); NR2B (ZK11), Invitrogen (for IP); synapsin (H-170), Santa Cruz; FLAG M2 and conjugated beads, Sigma; anti-GFP agarose, MBL. NR2B and NR2A antibodies for western blotting (C-terminal) were generous gifts from Richard Huganir. L-VNIO was from Alexis; NMDA and 2-bromopalmitate, Sigma.

Plasmids and Transfections

pgW.1-PSD-95-FLAG was a generous gift from David Bredt. Cysteine mutants and pgW.1-PSD-95-1-433-FLAG were generated using standard protocols for Phusion polymerase (Finnzymes). mEGFP-HRAS (Addgene plasmid 18662) was purchased from Addgene (Yasuda et al., 2006). Plasmids were transfected using polyfect (Qiagen) following manufacturer's instructions. For all experiments, cells were lysed 24 hr post-transfection.

Biotin-Switch Assay

Cell extracts or homogenates from age-matched mouse brain samples were analyzed by the biotin-switch assay as described with minor modifications (Jaffrey and Snyder, 2001). Briefly, 293 cells at 95% confluency or cerebellar granule cells seeded at 1 × 10 cells per dish were extracted in HEN buffer (in mM: 250 HEPES, 1 EDTA, 0.1 neocuproine, pH 7.7) containing 1% Triton X-100, 0.1% sodium deoxycholate, 0.1% SDS, 200 μM desferoxamine, with protease and phosphatase inhibitors (Sigma). Extracts were treated with methylmethanethiosulfonate (Sigma) in 2.5 % SDS at 50°C for 20 min. Proteins were precipitated with acetone and labeled with biotin-HPDP (0.8mM)(Pierce) with or without ascorbate (50 mM) for 90 min at room temperature. Proteins were precipitated twice with acetone and biotinylated proteins purified using neutravidin beads (Pierce), separated by SDS-PAGE, and analyzed by Western blotting.

Metabolic labeling with [^{3}H]palmitate

[^{3}H]palmitate was purchased from NEN and concentrated using a Speedvac. Cells were labeled in PBS with 0.1 mCi/mL palmitate (293 cells) or 0.5 mCi/mL palmitate in ACSF (neurons). Lysis was performed in modified RIPA buffer (50 mM Tris, 150 mM NaCl, 1 mM EDTA, 1% Triton X-100, 0.1% sodium deoxycholate, 0.1% SDS) and proteins of interest immunoprecipitated with the appropriate antibody overnight followed by a 2 hr incubation with protein A/G conjugated agarose (Calbiochem). Proteins were eluted at 70°C in Nupage sample buffer (2×) (Invitrogen) containing 1 mM DTT and separated on SDS-PAGE. For experiments with 293 cells, gels were stained with SimplyBlue (Invitrogen); for neuronal experiments, 10% of each eluate was western blotted for input controls. Gels for fluorography were soaked in Amplify (Amersham) for 30 min, dried under vacuum at 70°C, and exposed for 3–4 days (overexpressed protein) or 3–4 weeks (endogenous protein).

ABE Assay

Cell extracts or homogenates from age-matched brain samples were analyzed by the acyl-biotin exchange assay as described with minor modifications (Wan et al., 2007). Briefly, cells were lysed in buffer containing (in mM): 50 Tris, 50 NaCl, 1 EDTA, 2% SDS, supplemented with protease inhibitors. Extracts were sonicated briefly and treated with 10 mM NEM for 20 min at 37°C. Proteins were precipitated with acetone and labeled with biotin-HPDP (0.8mM) in buffer containing either 0.56M hydroxylamine pH 7.4 or 0.56M Tris pH 7.4 for 1 hour at room temperature. Proteins were run through a Zeba desalting column (Pierce) followed by acetone precipitation. Biotinylated proteins were purified using neutravidin beads (Pierce), separated by SDS-PAGE, and analyzed by Western blotting.

Immunostaining and Image Analysis

Neurons were seeded at a density of 1×10^6 cells/well onto polylysine coated Lab-Tek 2-well chamber slides. At 12 DIV, samples were treated with 100 μM NMDA in ACSF for 10 min with or without 100 μM VNIO pre-treatment (1 hr) and returned to normal media for 8 hr. Cells were fixed in 4% paraformaldehyde for 20 min, blocked in 5% goat serum with 0.1% Triton X-100 in PBS for 1 hr, and stained overnight at 4°C for PSD-95 (1:200) or synapsin (1:100) in blocking solution. Appropriate secondary antibodies conjugated to AlexaFluor 488 and 567 (Molecular Probes) were incubated with samples for 1 hr at room temperature following three washes with TBST. Slides were prepared using Fluormount G (Southern Biotech) and images taken with a Zeiss 510 Meta confocal microscope at 63×. Analysis of PSD-95 clusters was performed as described (Mukai et al., 2008). Briefly, the particle measurement function of ImageJ was used to count discrete fluorescent puncta in a proximal 20 μM section of the largest one or two dendrites per neuron. Settings of minimal punctum size and threshold were maintained constant across all treatment conditions. Pearson's coefficients were calculated using the colocalization threshold plugin for ImageJ.

Analysis of GluR2 Surface Clustering

Hippocampal neurons were treated with/without 20 μM 2-bromopalmitate for 8 hours. For live staining, neurons (DIV15) were incubated with anti-GluR2 N-terminal antibody (50mg/ml: Millipore) in conditioned medium for 15 min at 37°C. Neurons were fixed with 4% PFA for 10 min on ice, blocked in 5 mg/ml bovine serum albumin in PBS for 10 min and stained with secondary antibody under unpermeabilized conditions. Neurons were then permeabilized to detect the antigen. Images were taken with a confocal laser microscopy system (Carl Zeiss LSM 510; Carl Zeiss). The number of GluR2 fluorescencent puncta, which are merged with VGLUT1, was calculated as surface GluR2 using ImageJ. To quantitate changes in clustering, twelve fields were chosen from two independent neuronal cultures, and a largest proximal dendrite (30 mm long) was analyzed.

Co-immunoprecipitation

Proteins from brain homogenate were extracted with modified RIPA buffer and incubated with anti-NR2B antibody (Invitrogen) overnight followed by a 2 hr incubation with protein A/G agarose conjugated beads (Calbiochem). Beads were washed three times in modified RIPA, aspirated to dryness with a syringe, eluted with 2× LDS, and analyzed by SDS-PAGE.

Acknowledgments

We thank Michael Koldobskiy for helpful discussions and Masoumeh Saleh for maintaining and genotyping the nNOS knockout mice. This work was supported by US Public Health Service Grants MH18501 and Research Scientist Award DA-00074 (to S.H.S.), National Institutes of Health grant MH67068 (to J.A.G.), a Simons Foundation grant (to J.A.G.) and a NARSAD Young Investigator Award (to J.M.).

References

Aarts M, Liu Y, Liu L, Besshoh S, Arundine M, Gurd JW, Wang YT, Salter MW, Tymianski M. Treatment of ischemic brain damage by perturbing NMDA receptor- PSD-95 protein interactions. Science. 2002; 298:846–850. [PubMed: 12399596]

Beattie EC, Carroll RC, Yu X, Morishita W, Yasuda H, von Zastrow M, Malenka RC. Regulation of AMPA receptor endocytosis by a signaling mechanism shared with LTD. Nat Neurosci. 2000; 3:1291–1300. [PubMed: 11100150]

Beique JC, Lin DT, Kang MG, Aizawa H, Takamiya K, Huganir RL. Synapse-specific regulation of AMPA receptor function by PSD-95. Proc Natl Acad Sci U S A. 2006; 103:19535–19540. [PubMed: 17148601]

Bhattacharyya S, Biou V, Xu W, Schluter O, Malenka RC. A critical role for PSD-95/AKAP interactions in endocytosis of synaptic AMPA receptors. Nat Neurosci. 2009; 12:172–181. [PubMed: 19169250]

Bredt DS. Endogenous nitric oxide synthesis: biological functions and pathophysiology. Free Radic Res. 1999; 31:577–596. [PubMed: 10630682]

Bredt DS, Snyder SH. Nitric oxide mediates glutamate-linked enhancement of cGMP levels in the cerebellum. Proc Natl Acad Sci U S A. 1989; 86:9030–9033. [PubMed: 2573074]

Bredt DS, Snyder SH. Isolation of nitric oxide synthetase, a calmodulin-requiring enzyme. Proc Natl Acad Sci U S A. 1990; 87:682–685. [PubMed: 1689048]

Brenman JE, Chao DS, Gee SH, McGee AW, Craven SE, Santillano DR, Wu Z, Huang F, Xia H, Peters MF, et al. Interaction of nitric oxide synthase with the postsynaptic density protein PSD-95 and alpha1-syntrophin mediated by PDZ domains. Cell. 1996; 84:757–767. [PubMed: 8625413]

Chen L, Chetkovich DM, Petralia RS, Sweeney NT, Kawasaki Y, Wenthold RJ, Bredt DS, Nicoll RA. Stargazin regulates synaptic targeting of AMPA receptors by two distinct mechanisms. Nature. 2000; 408:936–943. [PubMed: 11140673]

Chen X, Winters C, Azzam R, Li X, Galbraith JA, Leapman RD, Reese TS. Organization of the core structure of the postsynaptic density. Proc Natl Acad Sci U S A. 2008; 105:4453–4458. [PubMed: 18326622]

Cho DH, Nakamura T, Fang J, Cieplak P, Godzik A, Gu Z, Lipton SA. S-nitrosylation of Drp1 mediates beta-amyloid-related mitochondrial fission and neuronal injury. Science. 2009; 324:102–105. [PubMed: 19342591]

Cho KO, Hunt CA, Kennedy MB. The rat brain postsynaptic density fraction contains a homolog of the Drosophila discs-large tumor suppressor protein. Neuron. 1992; 9:929–942. [PubMed: 1419001]

Choi YB, Tenneti L, Le DA, Ortiz J, Bai G, Chen HS, Lipton SA. Molecular basis of NMDA receptor-coupled ion channel modulation by S-nitrosylation. Nat Neurosci. 2000; 3:15–21. [PubMed: 10607390]

Christopherson KS, Hillier BJ, Lim WA, Bredt DS. PSD-95 assembles a ternary complex with the N-methyl-D-aspartic acid receptor and a bivalent neuronal NO synthase PDZ domain. J Biol Chem. 1999; 274:27467–27473. [PubMed: 10488080]

Craven SE, El-Husseini AE, Bredt DS. Synaptic targeting of the postsynaptic density protein PSD-95 mediated by lipid and protein motifs. Neuron. 1999; 22:497–509. [PubMed: 10197530]

Drisdel RC, Alexander JK, Sayeed A, Green WN. Assays of protein palmitoylation. Methods. 2006; 40:127–134. [PubMed: 17012024]

el-Husseini Ael D, Bredt DS. Protein palmitoylation: a regulator of neuronal development and function. Nat Rev Neurosci. 2002; 3:791–802. [PubMed: 12360323]

El-Husseini Ael D, Schnell E, Dakoji S, Sweeney N, Zhou Q, Prange O, Gauthier-Campbell C, Aguilera-Moreno A, Nicoll RA, Bredt DS. Synaptic strength regulated by palmitate cycling on PSD-95. Cell. 2002; 108:849–863. [PubMed: 11955437]

Eliasson MJ, Blackshaw S, Schell MJ, Snyder SH. Neuronal nitric oxide synthase alternatively spliced forms: prominent functional localizations in the brain. Proc Natl Acad Sci U S A. 1997; 94:3396–3401. [PubMed: 9096405]

Fukata Y, Fukata M. Protein palmitoylation in neuronal development and synaptic plasticity. Nat Rev Neurosci. 2010; 11:161–175. [PubMed: 20168314]

Ge X, Jin Q, Zhang F, Yan T, Zhai Q. PCAF acetylates {beta}-catenin and improves its stability. Mol Biol Cell. 2009; 20:419–427. [PubMed: 18987336]

Giandomenico V, Simonsson M, Gronroos E, Ericsson J. Coactivator-dependent acetylation stabilizes members of the SREBP family of transcription factors. Mol Cell Biol. 2003; 23:2587–2599. [PubMed: 12640139]

Gronroos E, Hellman U, Heldin CH, Ericsson J. Control of Smad7 stability by competition between acetylation and ubiquitination. Mol Cell. 2002; 10:483–493. [PubMed: 12408818]

Hancock JF, Magee AI, Childs JE, Marshall CJ. All ras proteins are polyisoprenylated but only some are palmitoylated. Cell. 1989; 57:1167–1177. [PubMed: 2661017]

Hayashi T, Thomas GM, Huganir RL. Dual palmitoylation of NR2 subunits regulates NMDA receptor trafficking. Neuron. 2009; 64:213–226. [PubMed: 19874789]

Hess DT, Matsumoto A, Kim SO, Marshall HE, Stamler JS. Protein S-nitrosylation: purview and parameters. Nat Rev Mol Cell Biol. 2005; 6:150–166. [PubMed: 15688001]

Hess DT, Patterson SI, Smith DS, Skene JH. Neuronal growth cone collapse and inhibition of protein fatty acylation by nitric oxide. Nature. 1993; 366:562–565. [PubMed: 8255294]

Huang PL, Fishman MC. Genetic analysis of nitric oxide synthase isoforms: targeted mutation in mice. J Mol Med. 1996; 74:415–421. [PubMed: 8872855]

Jaffrey SR, Erdjument-Bromage H, Ferris CD, Tempst P, Snyder SH. Protein S-nitrosylation: a physiological signal for neuronal nitric oxide. Nat Cell Biol. 2001; 3:193–197. [PubMed: 11175752]

Jaffrey SR, Snyder SH. The biotin switch method for the detection of S-nitrosylated proteins. Sci STKE. 2001; 2001:pl1. [PubMed: 11752655]

Kang BN, Ahmad AS, Saleem S, Patterson RL, Hester L, Dore S, Snyder SH. Death-associated protein kinase-mediated cell death modulated by interaction with DANGER. J Neurosci. 2010; 30:93–98. [PubMed: 20053891]

Kang R, Wan J, Arstikaitis P, Takahashi H, Huang K, Bailey AO, Thompson JX, Roth AF, Drisdel RC, Mastro R, et al. Neural palmitoyl-proteomics reveals dynamic synaptic palmitoylation. Nature. 2008; 456:904–909. [PubMed: 19092927]

Kato AS, Zhou W, Milstein AD, Knierman MD, Siuda ER, Dotzlaf JE, Yu H, Hale JE, Nisenbaum ES, Nicoll RA, et al. New transmembrane AMPA receptor regulatory protein isoform, gamma-7, differentially regulates AMPA receptors. J Neurosci. 2007; 27:4969–4977. [PubMed: 17475805]

Lander HM, Milbank AJ, Tauras JM, Hajjar DP, Hempstead BL, Schwartz GD, Kraemer RT, Mirza UA, Chait BT, Burk SC, et al. Redox regulation of cell signalling. Nature. 1996; 381:380–381. [PubMed: 8632794]

Li B, Otsu Y, Murphy TH, Raymond LA. Developmental decrease in NMDA receptor desensitization associated with shift to synapse and interaction with postsynaptic density-95. J Neurosci. 2003; 23:11244–11254. [PubMed: 14657184]

Migaud M, Charlesworth P, Dempster M, Webster LC, Watabe AM, Makhinson M, He Y, Ramsay MF, Morris RG, Morrison JH, et al. Enhanced long-term potentiation and impaired learning in mice with mutant postsynaptic density-95 protein. Nature. 1998; 396:433–439. [PubMed: 9853749]

Mukai J, Dhilla A, Drew LJ, Stark KL, Cao L, MacDermott AB, Karayiorgou M, Gogos JA. Palmitoylation-dependent neurodevelopmental deficits in a mouse model of 22q11 microdeletion. Nat Neurosci. 2008; 11:1302–1310. [PubMed: 18836441]

Mukai J, Liu H, Burt RA, Swor DE, Lai WS, Karayiorgou M, Gogos JA. Evidence that the gene encoding ZDHHC8 contributes to the risk of schizophrenia. Nat Genet. 2004; 36:725–731. [PubMed: 15184899]

Mustafa AK, Gadalla MM, Sen N, Kim S, Mu W, Gazi SK, Barrow RK, Yang G, Wang R, Snyder SH. H2S signals through protein S-sulfhydration. Sci Signal. 2009; 2:ra72. [PubMed: 19903941]

Noritake J, Fukata Y, Iwanaga T, Hosomi N, Tsutsumi R, Matsuda N, Tani H, Iwanari H, Mochizuki Y, Kodama T, et al. Mobile DHHC palmitoylating enzyme mediates activity-sensitive synaptic targeting of PSD-95. J Cell Biol. 2009; 186:147–160. [PubMed: 19596852]

Sattler R, Xiong Z, Lu WY, Hafner M, MacDonald JF, Tymianski M. Specific coupling of NMDA receptor activation to nitric oxide neurotoxicity by PSD-95 protein. Science. 1999; 284:1845–1848. [PubMed: 10364559]

Schnell E, Sizemore M, Karimzadegan S, Chen L, Bredt DS, Nicoll RA. Direct interactions between PSD-95 and stargazin control synaptic AMPA receptor number. Proc Natl Acad Sci U S A. 2002; 99:13902–13907. [PubMed: 12359873]

Selvakumar B, Huganir RL, Snyder SH. S-nitrosylation of stargazin regulates surface expression of AMPA-glutamate neurotransmitter receptors. Proc Natl Acad Sci U S A. 2009; 106:16440–16445. [PubMed: 19805317]

Stein V, House DR, Bredt DS, Nicoll RA. Postsynaptic density-95 mimics and occludes hippocampal long-term potentiation and enhances long-term depression. J Neurosci. 2003; 23:5503–5506. [PubMed: 12843250]

Sturgill JF, Steiner P, Czervionke BL, Sabatini BL. Distinct domains within PSD-95 mediate synaptic incorporation, stabilization, and activity-dependent trafficking. J Neurosci. 2009; 29:12845–12854. [PubMed: 19828799]

Takahashi H, Shin Y, Cho SJ, Zago WM, Nakamura T, Gu Z, Ma Y, Furukawa H, Liddington R, Zhang D, et al. Hypoxia enhances S-nitrosylation-mediated NMDA receptor inhibition via a thiol oxygen sensor motif. Neuron. 2007; 53:53–64. [PubMed: 17196530]

Topinka JR, Bredt DS. N-terminal palmitoylation of PSD-95 regulates association with cell membranes and interaction with K+ channel Kv1.4. Neuron. 1998; 20:125–134. [PubMed: 9459448]

Wan J, Roth AF, Bailey AO, Davis NG. Palmitoylated proteins: purification and identification. Nat Protoc. 2007; 2:1573–1584. [PubMed: 17585299]

Whalen EJ, Foster MW, Matsumoto A, Ozawa K, Violin JD, Que LG, Nelson CD, Benhar M, Keys JR, Rockman HA, et al. Regulation of beta-adrenergic receptor signaling by S-nitrosylation of G-protein-coupled receptor kinase 2. Cell. 2007; 129:511–522. [PubMed: 17482545]

Yasuda R, Harvey CD, Zhong H, Sobczyk A, van Aelst L, Svoboda K. Supersensitive Ras activation in dendrites and spines revealed by two-photon fluorescence lifetime imaging. Nat Neurosci. 2006; 9:283–291. [PubMed: 16429133]

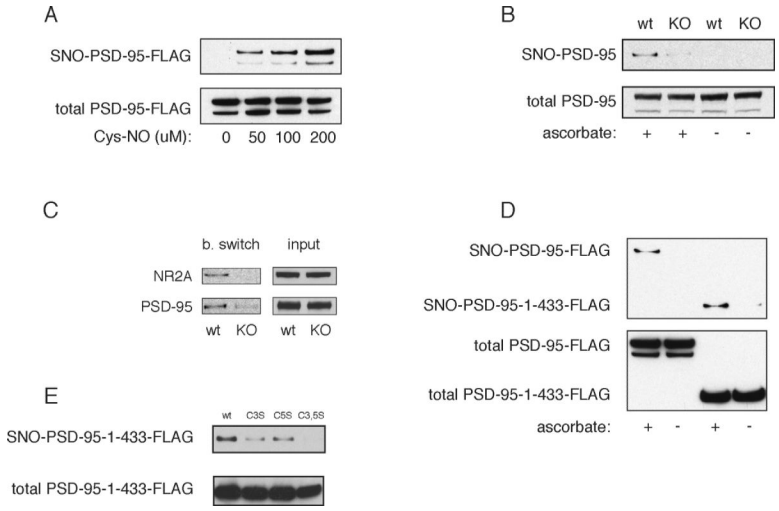

Figure 1. PSD-95 is nitrosylated on C3 and C5

(A) Nitrosylation of PSD-95 in heterologous cells. HEK293 cells were transfected with PSD-95-FLAG, treated with the indicated concentrations of Cys-NO for 5 min, and analyzed by the biotin switch.

(B) Basal nitrosylation of endogenous PSD-95 in mouse brain demonstrated by abolition of the biotin switch SNO-PSD-95 signal in nNOS−/− brain homogenate when compared to wild type. Ascorbate dependence demonstrates specificity of the signal.

(C) Basal nitrosylation of endogenous PSD-95 and NR2A in mouse brain demonstrated by abolition of the biotin switch SNO-PSD-95 signal in nNOS−/− brain homogenate when compared to wild type. Both proteins are nitrosylated at comparable levels.

(D) Nitrosylation of PSD-95-C3, C5 by physiologically generated NO. HEK-nNOS cells were transfected with either full length PSD-95 or truncated (PSD-95-1-433-FLAG, containing PDZ1-3), and analyzed by the biotin switch assay. The SNO-PSD-95-1-433 signal demonstrates nitrosylation of C3, C5, as these are the only two cysteines present in the fragment.

(E) Nitrosylation of single cysteine mutants. HEK-nNOS cells transfected with wild type or the indicated mutants of PSD-95-1-433-FLAG were analyzed by the biotin switch.

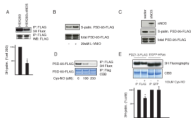

Figure 2. Nitric oxide inhibits PSD-95 palmitoylation in heterologous cells

(A) nNOS expression correlates with decreased palmitoylation of PSD-95. HEK293 or HEK-nNOS cells were transfected with PSD-95-FLAG and metabolically labeled with [^{3}H]palmitate. Immunoprecipitation (IP) and detection of incorporated [^{3}H] into PSD-95-FLAG (top panel). Input and expression were confirmed by western blot (WB, bottom panel). Representative result (top). Quantification (bottom). Palmitoylated PSD-95 was measured by scanning densitometry, normalized to input, and expressed as a percentage of the untreated sample. Data are means±SEM (n=3). *, $p < 0.02$ by Student's t-test relative to untreated.

(B) Pharmacologic nNOS inhibition in HEK-nNOS cells increases PSD-95 palmitoylation. HEK-nNOS cells transiently transfected with PSD-95-FLAG were treated with 20 μM L-VNIO overnight and PSD-95 palmitoylation was measured by the ABE assay.

(C) nNOS expression correlates with decreased palmitoylation of PSD-95. HEK293 cells were co-transfected with PSD-95-FLAG and either nNOS or empty vector control. PSD-95 palmitoylation was measured by the ABE assay.

(D) Concentration-dependent inhibition of palmitoylation of PSD-95 by Cys-NO. HEK293 cells expressing PSD-95-FLAG were metabolically labeled with [H]palmitate followed by FLAG IP, coomassie (CBB) stain and fluorography of the same gel.

(E) Specificity of NO mediated inhibition of palmitoylation. HEK293 cells were co-transfected with PSD-95-1-433-FLAG and mEGFP-HRas and analyzed as in (D). Representative result (top). Quantification (bottom), analyzed as in (A). n=3, *, $p < 0.05$.

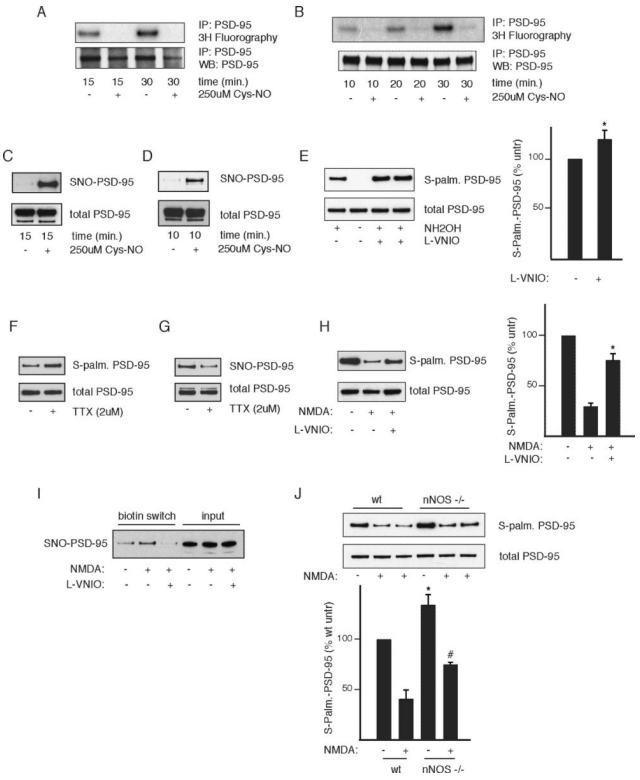

Figure 3. Nitric oxide inhibits endogenous PSD-95 in neurons

(A and B) Cys-NO inhibits palmitoylation of endogenous PSD-95. Cerebellar granule (A) or hippocampal (B) neurons were metabolically labeled in the presence or absence of 250 μM Cys-NO and analyzed as in Figure 2A.

(C and D) Cys-NO elicits nitrosylation of endogenous PSD-95. Cerebellar granule (C) or hippocampal (D) neuronal cultures were subjected to the biotin switch assay following treatment with Cys-NO as in Figure 3A and B.

(E) L-VNIO treatment increases basal PSD-95 palmitoylation. Cerebellar granule cells were treated with 75 μM L-VNIO for 8 hr to inhibit nNOS and subjected to the ABE assay. Hydroxylamine (NH OH) dependence indicates specificity of the signal. Representative result (left). Quantification (right), analyzed as in (A). n=4, *, $p < 0.04$.

(F) TTX increases PSD-95 palmitoylation. Cerebellar granule cells were treated with 2 μM TTX for 4 hr in conditioned media and analyzed by the ABE assay.

(G) TTX decreases PSD-95 nitrosylation. Cerebellar granule cells were treated as in (F) and analyzed by the biotin switch assay.

(H) NMDA decreases PSD-95 palmitoylation in an NO-dependent manner. Cerebellar granule cells were treated with 300 μM NMDA and 10 μM glycine in ACSF for 10 min with or without 1 hr of 75 μM VNIO pre-treatment, returned to normal media for 8 hr, and analyzed by ABE. Representative result (left). Quantification (right), analyzed as in (E). n=3, *, $p < 0.02$ relative to NMDA treated.

(I) NMDA elicits PSD-95 nitrosylation in an NO-dependent manner. Nitrosylation of PSD-95 in cerebellar granule cells was measured by the biotin switch assay following treatment with NMDA and/or VNIO as in Figure 3H.

(J) Increased PSD-95 palmitoylation in nNOS−/− cultures. Cerebellar granule cells derived from either wild type or nNOS−/− mice were treated with NMDA as in (H) and analyzed by ABE. Representative result (top); quantification (bottom), analyzed as in (F). n=4, *, $p < 0.05$ relative to untreated wt; #, $p < 0.02$ relative to wt + NMDA.

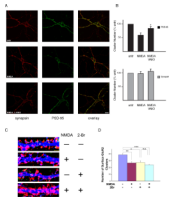

Figure 4. NO inhibits PSD-95 clustering

(A) Representative images of PSD-95 clusters (green) and their localization in synapsin (red) labeled cerebellar granule neurons at DIV12. Cells were treated with 100 μM NMDA in ACSF with or without 1 hr 100 μM L-VNIO pre-treatment. Scale bar, 10 μm.

(B) Reduction in the number of PSD-95 clusters with NMDA partially reversed by L-VNIO. Quantified data were generated as described in Experimental Procedures. Data are expressed as means ±SEM. *, $p < 0.02$ relative to NMDA treated by Student's t-test.

(C) Representative images of the dendritic expression of live stained surface GluR2 using a N-terminal antibody (*green*) and VGLUT1 (*red*) in MAP2 (*blue*) labeled hippocampal neurons at DIV15. Neurons were treated with/without 20 μM 2-BP for 8 hours and then treated with/without 100 μM NMDA for 10 min. Scale bar: 2 μm.

(D) Reduction in the number of surface GluR2 clusters with 2-BP treatment is not further increased by NMDA treatment. Quantified data were generated as described in Experimental Procedures.

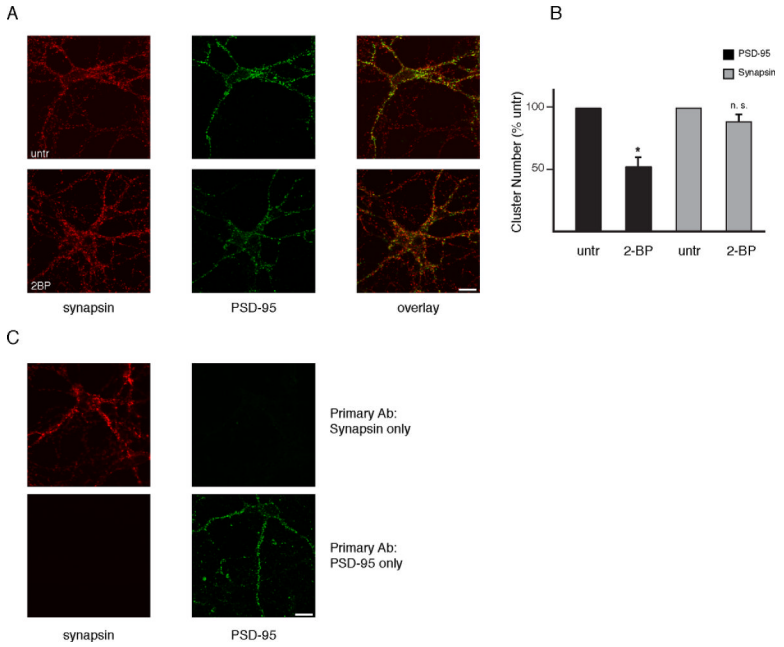

Figure 5. Effects of 2-bromopalmitate on PSD-95 and specificity of double immunostaining

(A) Representative images of PSD-95 clusters (green) and their localization in synapsin (red) labeled cerebellar granule neurons at DIV12. Cells were treated with 10 μM 2-BP in conditioned media for 8 hr. Scale bar, 10 μm.

(B) Reduction in the number of PSD-95 clusters with 2-BP treatment. Quantified data were generated as in Figure 4. *, $p < 0.001$ relative to untreated by Student's t-test.

(C) Verification of double immunolabeling specificity. Cells were stained as in Figure 4 with omission of either PSD-95 or synapsin primary antibody.

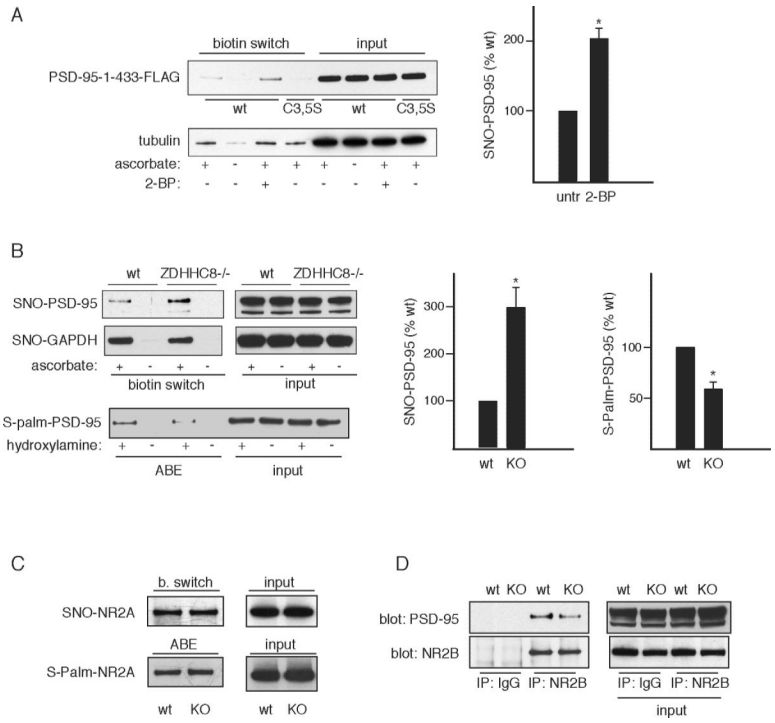

Figure 6. Palmitoylation regulates PSD-95 nitrosylation

(A) 2-BP treatment of HEK-nNOS cells increases nitrosylation. HEK-nNOS cells expressing PSD-95-1-433-FLAG or the corresponding C3, C5S mutant were treated with 100 μM 2-BP for 4 hr and analyzed by biotin switch. β-tubulin is a control nitrosylated protein unaffected by 2BP treatment. Left, representative result. Right, quantification of nitrosylated PSD-95-1-433-FLAG, analyzed as in Figure 2. n=3, *, $p < 0.02$ relative to untreated.

(B) ZDHHC8−/− mice have increased endogenous SNO-PSD-95. Brain homogenates from age-matched wt or ZDHHC8−/− mice were analyzed by biotin switch and ABE. Left, representative result. Middle, quantification for the biotin switch, analyzed as in (A). n=3, *, $p < 0.04$ relative to wild type. Right, quantification for ABE, n=3, *, $p < 0.05$ relative to wild type. GAPDH nitrosylation is also demonstrated but does not increase in the ZDHHC−/− mouse.

(C) Basal nitrosylation of NR2A was demonstrated in wild type and ZDHHC8−/− mouse brain by the biotin switch assay. Palmitoylation was measured by the ABE assay.

(D) Decreased binding of NR2B to PSD-95 in ZDDHC−/− mice. NR2B was immunoprecipitated from ZDHHC−/− or wild type brain homogenate and blotted for PSD-95.

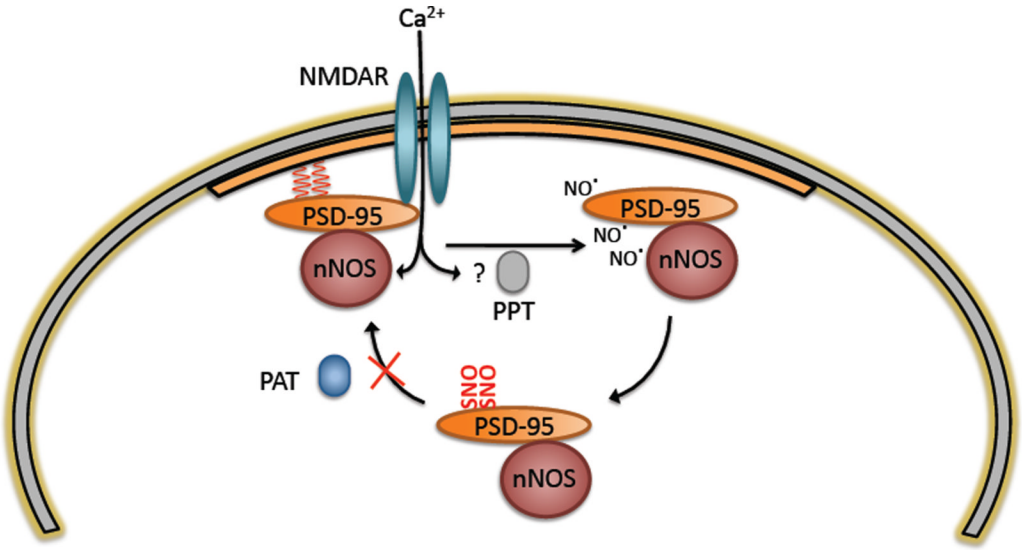

Figure 7. Model for NO mediated regulation of PSD-95 synaptic targeting

While palmitoylated (red wavy lines), PSD-95 is stably associated with the PSD (orange region). NMDA stimulation promotes de-palmitoylation through a putative palmitoyl protein thioesterase (PPT) (El-Husseini Ael et al., 2002). Simultaneously, calcium entering cells through the NMDA ion channel activates nNOS by binding to calmodulin, causing NO formation. NO generated in close proximity to PSD-95 nitrosylates PSD-95, blocking free cysteines and preventing re-palmitoylation by PSD-95 PATs and subsequent association with the PSD.